

SPATIAL AND TEMPORAL STRUCTURE OF A TIME DEPENDENT PIPE FLOW

Y. Sato*, Y. Takeda*, D. Sugiyama*

* Div. of Mechanical Science, Graduate School of Engineering, Hokkaido University, Kita-13 Nishi-8, Sapporo, Japan,
E-mail: yohei@ring-me.eng.hokudai.ac.jp

ABSTRACT

Time dependent velocity distribution of an oscillating pipe flow has been measured by ultrasound Doppler method. Velocity field showed typical pulsatile flow nature as totally different from a stationary pipe flow.

Time domain Fourier transfer was used to obtain temporal characteristics of this flow, as being space dependent power spectrum. By decomposing temporal characteristics and analyzing their spatial dependence of each model, we found the energy is more concentrated in the boundary region (named as HPA – Higher Power Area), and it appears that turbulence starts to be generated in this area by increasing Reynolds number.

Keywords: Oscillating flow, Spacio-temporal Measurement, Weakly Turbulent flow, HPA

INTRODUCTION

The theoretical solution of purely oscillating flow was determined by Uchida [1], and Annular Effect was known as preceding of the phase near the wall of the pipe. Experiments on oscillating pipe flow have been carried out by Christian von Kerczek [2] for the Stokes layer in oscillating flow and Merkli & Thoman [3], Hino [4] for transition to turbulent flow.

In earlier experiments, it was possible to measure at only one spatial point at the same time. In this experiment, Ultrasonic Doppler Method (UDM) made possible measurement on a line at the same time. The spatial structure of the oscillating pipe flow can be available with UDM.

STABILITY DIAGRAM

Figure 1 shows the stability diagram of purely oscillating pipe flow. The types of oscillating pipe flow can be classified in terms of the Reynolds number R_δ and Stokes parameter λ into laminar flow, weakly turbulent flow and conditionally turbulent flow. In weakly turbulent flow, turbulence is generated weekly. In conditionally turbulent flow, turbulence is generated suddenly in the decelerating phase. R_δ is defined as $R_\delta = U\delta/\nu$ using the Stokes-layer thickness $\delta = (2\nu/\omega)^{1/2}$ and the cross-sectional mean velocity amplitude $U = A\omega$. λ is defined as $\lambda = 1/2d(\omega/2\nu)^{1/2}$. (ν =kinematic viscosity, ω =angular frequency, A =amplitude and d =inner diameter of the pipe)

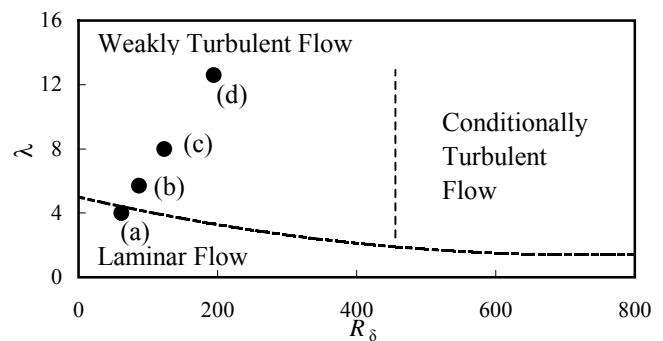


Figure 1. Stability Diagram, Hino *et al.* [4]

EXPERIMENTAL ARRANGEMENT

The general arrangement of the equipment is shown in Figure 2. The pipe is connected to the reservoir at one end. The oscillations are driven by an oscillating piston at the other end.

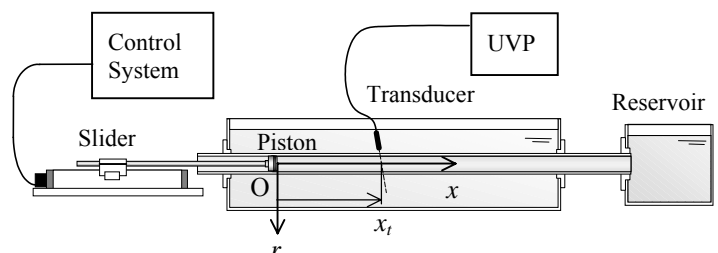


Figure 2. Experimental arrangement and coordinate axis

A liner motion stepping motor makes the monotonic oscillation of piston. The pipe has an inner diameter of 26 mm and a length of 2000 mm. The measuring section is in a large water tank to prevent changing of temperature.

Velocity was measured by Ultrasonic Velocity Profiler (UVP) with a basic frequency 4 MHz. The transducer is fixed above the pipe with an angle of 78° between the ultrasonic beam axis and the pipe axis. The tracer is Grilex5P1 ($\rho=1.05\text{g/cm}^3$). 20 % Glycerol-water solution is used for the fluid to make the density of fluid closer to the density of the tracer.

Coordinate axes are shown in Figure 2. The origin O is set on the center of the pipe. The x -axis has the direction of the axis of the pipe. The r -axis has the direction of the radius of the pipe. The x -component of the piston x_i is the intersection of the x -axis and the ultrasonic beam axis.

The piston moves with sin-wave $x=A \sin \omega t$ (x =position of piston head, A =amplitude of sin-wave, ω =angular frequency and t =time). A was kept constant $A=100$ [mm]. ω was set at 0.31, 0.62, 1.25 and 3.14 [rad]. Then $R_\delta=61.5, 87.0, 123.0$ and 194.5 and $\lambda=4.0, 5.7, 8.0$ and 12.6 (Figure. 1 (a) ~ (d)). The measuring points are set every $\Delta r/D=0.028$ from $r/D=-0.5$ to $r/D=0.5$ every $\Delta x/D=0.769$ from $x/D=5$ to $x/D=23.4$.

EXPERIMENTAL RESULTS AND ANALYSIS

Figure 3 shows an example of an instantaneous velocity profile in the accelerating phase. The velocity near the wall is higher than center (Annular effect). Figure 4 is a typical example of the velocity-time series at one spatial point showing a regular sinusoidal motion.

Each time series data was analyzed by FFT in order to see the temporal characteristics of the flow.

Then, analyzed data was averaged over x -axis for $5 < x/D < 23.4$. The space dependent power spectra are shown in Figure 5 for various Reynolds number. The coordinate is the radial position and the abscissa is frequency. The collar represents the magnitude of the power. These graphs show the distribution of the power on the r -axis. The power of the base frequency is much higher than the others at every position. When R_δ and λ are increased, the higher order harmonics can be recognized clearly especially near the wall.

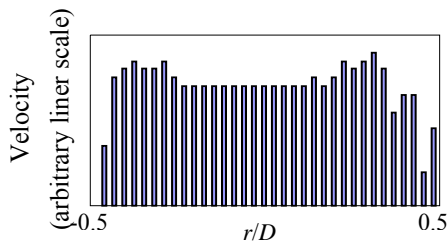


Figure 3. Example of velocity profile ($R_\delta=123.0, \lambda=8.0, x/D=21.15, \theta=1.3\pi$)

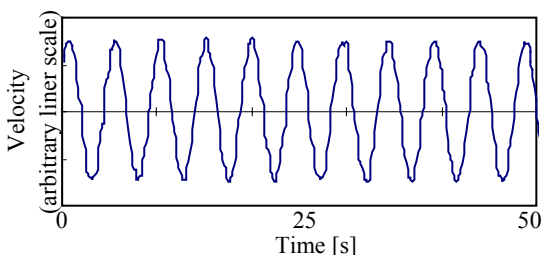


Figure 4. Example of velocity-time series ($R_\delta=123.0, \lambda=8.0, x/D=21.15, r/D=0$)

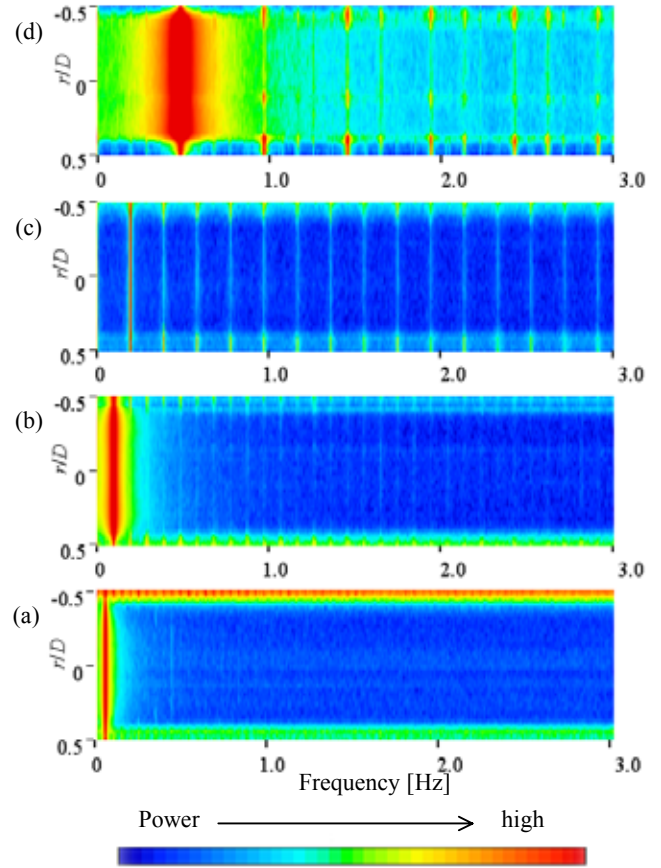


Figure 5. Space dependent power spectrum
(a) $R_\delta=61.5, \lambda=4.0$ (b) $R_\delta=87.0, \lambda=5.7$
(c) $R_\delta=123.0, \lambda=8.0$ (d) $R_\delta=194.5, \lambda=12.6$

DISCUSSION

Figure 6 shows the spatial distribution of the power of the base frequency at various Reynolds number. The distribution has one broad peak in the inner region of the pipe at $R_\delta=61.5, \lambda=4.0$ (a). The distribution has two peaks outside of the central region at $R_\delta=87.0, \lambda=5.7$ (b). We call those peaks Higher Power Area (HPA). Two HPAs appear too at $R_\delta=123.0, \lambda=8.0$ (c). But the location is closer to the wall and the space between each HPA is wider than (b). The distribution looks like a trapezoid at $R_\delta=194.5, \lambda=12.6$ (d). For all cases power is lower just next to the wall.

Figure 7 shows the similar spatial distribution of the power of the second harmonic mode. Two HPAs appear near the wall, but their location is closer to the wall than that of the base frequency. The distribution looks almost flat in the inner region for all cases.

The case (a) corresponds to laminar flow according to Hino [4] and Fig.1. The spatial distribution of the base frequency is higher in the inner region. This seems reasonable since oscillation is driven by a sinusoidal motion of the piston and the energy is given to fluid uniformly. On contrary for (c) to (d), Most of the power is distributed near the wall. This indicates that this mode is generated by being caused by a boundary layer. It may be considered that the energy of the basic mode is transferred to this higher harmonic mode inside

this boundary layer, and as a result, the power of the base frequency is much lower than in the inner region.

From this result, flow transition from laminar to turbulent flow might be defined as following. For laminar flow the energy is concentrated only on the basic mode and there is no HPA of the fundamental frequency and are the power of the higher harmonic mode is low. When R_δ and λ are increased, HPA appears with fundamental frequency outside of the central region as well as for the higher harmonic mode. The HPA of harmonic mode appears just next to the wall at (b) and is moving to the central region of the pipe by increasing R_δ . The power itself appears to increase. Consequently, the flow is considered to transit to weakly turbulent flow.

This result also indicates that the boundary layer is given the energy from the basic mode through the higher harmonic mode by nonlinear mechanisms because the power of fundamental mode is lower relative to other region and that of the harmonic frequency is higher near the wall. In other word, the fact that the power of fundamental frequency is higher near the wall when R_δ and λ are increased means the flow in this area is following the motion of the piston more faithfully. It corresponds to see the annular effect. However when R_δ and λ are small, the peak of the power of base frequency is at the center. Annular Effect may not be seen in laminar flow.

CONCLUSION

Spatial and temporal characteristics of the oscillating pipe flow was investigated. From the space dependent power

spectra, flow transition might be defined using the appearance of HPA and the behavior of their location. The transition scheme observed seems to support the earlier investigation. It suggests a possible future work on the flow transition based on the energy transfer among various harmonic modes.

REFERENCES

1. Uchida S. The pulsating viscous flow superposed on the steady laminar motion of incompressible fluid in a circular pipe: *Z. Angew. Math. Phys.* 1956, **7**, 403-422
2. Kerczek CV and Davis SH: Liner stability theory of oscillatory Stokes layers , *J. Fluid Mech.* 1974, **62** (4), 193-207
3. Merkli P and Thomann H: Transition to turbulence in oscillating pipe flow , *J. Fluid Mech.* 1975, **68** (3), 567-575
4. Hino M, Sawamoto M, Takasu S: Experiments on transition to turbulence in an oscillatory pipe flow , *J. Fluid Mech.* 1976, **75** (2), 193-207
5. Elkholy AH. Sinusoidal excitation of viscous fluids in pipes: *Int. J. Pres. Ves. & Piping* 70 1997, 161-165

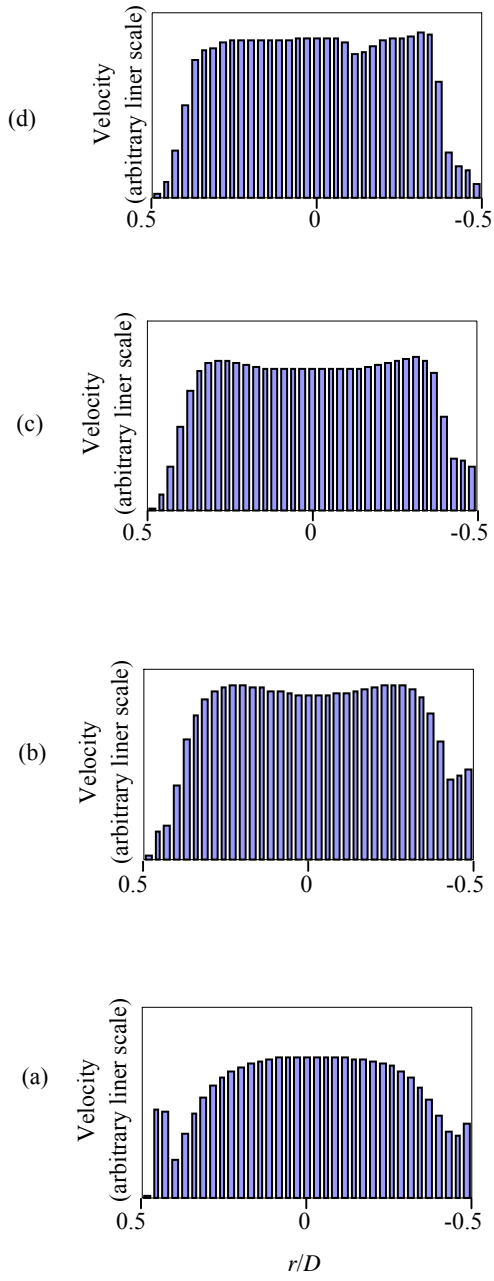


Figure 6. Spatial distribution of the power of base frequency
 (a) $R_\delta=61.5, \lambda=4.0$ (b) $R_\delta=87.0, \lambda=5.7$
 (c) $R_\delta=123.0, \lambda=8.0$ (d) $R_\delta=194.5, \lambda=12.6$

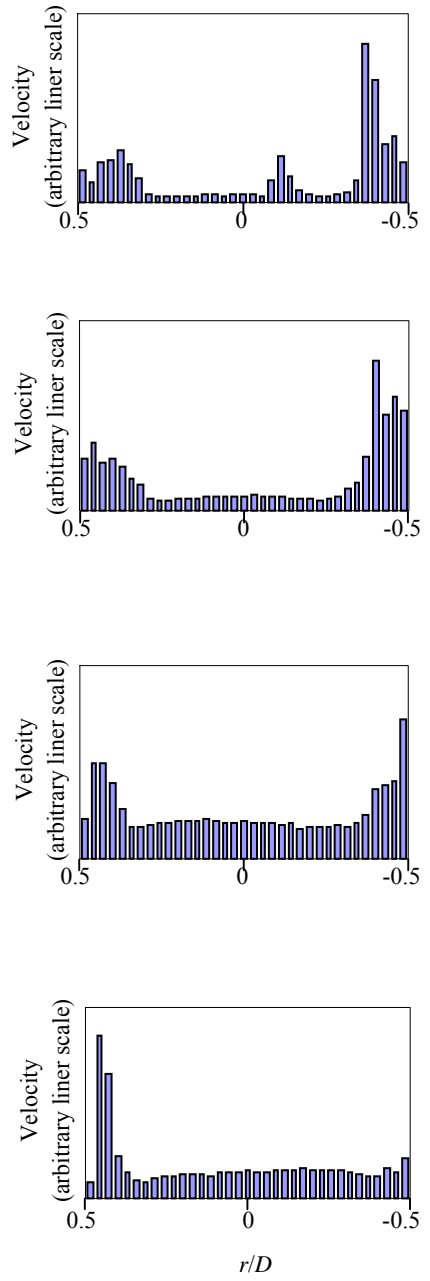


Figure 7. Spatial distribution of the power of second harmonic
 (a) $R_\delta=61.5, \lambda=4.0$ (b) $R_\delta=87.0, \lambda=5.7$
 (c) $R_\delta=123.0, \lambda=8.0$ (d) $R_\delta=194.5, \lambda=12.6$